Biochemistry

 Volume 34, Number 19 May 16, 1995

Accelerated Publications

The Peptide-Binding Domain of the Chaperone Protein Hsc70 Has an Unusual Secondary Structure Topology†

Robert C. Morshauser,‡ Hong Wang,§ Gregory C. Flynn,|| and Erik R. P. Zuiderweg*,‡,§

Department of Biological Chemistry and Biophysics Research Division, The University of Michigan, 930 North University Avenue, Ann Arbor, Michigan 48109, and Institute of Molecular Biology, Klamath Hall, University of Oregon, Eugene, Oregon 97403

Received February 23, 1995; Revised Manuscript Received April 4, 1995®

ABSTRACT: Modern NMR methods were used to determine the secondary structure topology of the 18 kDa peptide binding domain of the chaperone protein Hsc70 in solution. This report constitutes the first experimental conformational information on this important domain of the class of Hsp70 proteins. The domain consists of two four-stranded antiparallel β-sheets and a single α-helix. The topology does not resemble at all the topology observed in the human leukocyte antigen (HLA) proteins of the major histocompatibility complex. This is significant because such resemblance was predicted on the basis of limited amino acid homology, secondary structure prediction, and related function. Moreover, the exact meander-type β-sheet topology identified in Hsc70 has to our best knowledge not been observed in any other known protein structure.

Heat shock cognate protein (Hsc70)[1] is a member of the highly conserved 70 kDa heat shock (Hsp70) family of proteins, found in species ranging from bacteria to mammals (Lindquist, 1987). A wide variety of roles have been proposed for Hsp70 members, including clathrin vesicle uncoating, dissociating protein aggregates, facilitating protein translocation, and chaperoning protein folding in various cellular compartments. In all these proposed roles, Hsp70s bind directly to unfolded or partially folded polypeptide chains. Because of their suggested roles in protein folding, Hsp70s have been classified as molecular chaperones [see Craig et al. (1993) for a introductory review].

Peptide binding studies indicate that Hsp70s interact with extended, thus unfolded, hydrophobic structures (Flynn et al., 1989, 1991; Blond-Elguindi et al., 1993; Landry et al., 1992; Palleros et al., 1991; Gragerov & Gottesman, 1994). Peptide or polypeptide binding stimulates the weak ATPase activity of Hsp70s (Braell et al., 1984; Flynn et al., 1989). Rothman and co-workers (Chappel et al., 1986) subjected Hsc70 to limited proteolysis, obtaining a 60 kDa N-terminal fragment which was further cleaved to a 44 kDa N-terminal fragment. The 60 kDa fragment retained the ability to bind clathrin but was incapable of coupling the energy of ATP hydrolysis to clathrin uncoating. The 44 kDa N-terminal domain possessed an unregulated ATPase activity and was thus termed the "ATPase core". The three-dimensional structure of the ATPase core of Hsc70 was determined by

† Supported by a University of Michigan Rackham Research Partnership to R.C.M. and E.R.P.Z. and by American Cancer Society Grant NP-848 to G.C.F.

* To whom correspondence should be addressed [Fax, (+) (313) 764-3323; E-mail, erpz@ernst.biop.umich.edu].

‡ Department of Biological Chemistry, The University of Michigan.

§ Biophysics Research Division, The University of Michigan.

|| Institute of Molecular Biology, University of Oregon.

® Abstract published in *Advance ACS Abstracts,* May 1, 1995.

[1] Abbreviations: Hsp, heat shock protein; Hsc, heat shock cognate; HLA, human leukocyte antigen; MHC-I, major histocompatibility complex, class I; PBD, peptide binding domain; NOE, nuclear Overhauser effect.

0006-2960/95/0434-6261$09.00/0

X-ray diffraction methods; the structure is very reminiscent of the ATP binding domains of G-actin and hexokinase (Flaherty et al., 1990). This 44 kDa N-terminal domain does not, however, bind to unfolded proteins, peptides, or clathrin. The results of Chappell et al. demonstrated that the middle 16 kDa polypeptide directly adjacent to the 44 kDa ATPase core of Hsc70 was necessary for clathrin, and correspondingly peptide, binding. These results likewise demonstrated that the C-terminal fragment of the full Hsc70 protein was not required for clathrin (hence peptide) binding. More recently, the peptide binding activity was directly shown to reside exclusively within the isolated middle 18 kDa fragment immediately following the 44 kDa ATP binding domain (Wang et al., 1993). Wang and co-workers found this Hsc70 fragment to have an affinity (8 μM) indistinguishable from that of native Hsc70 (5−8 μM) for the S-peptide of RNase A. They also expressed a larger C-terminal domain, Hsc386−end, in tandem with glutathione transferase, and found the same peptide affinity. Thus, it follows that all peptide binding determinants are located in the 18 kDa fragment directly adjacent to the ATP binding fragment.

Because of the similarity in function, size, and limited amino acid homology, the peptide binding domain of Hsp70 has been modeled on the basis of the human leukocyte antigen (HLA) peptide-presenting protein of MHC-I (Rippmann et al., 1991; Flajnik et al., 1991). We report here the experimental determination of the secondary structure topology of the 18 kDa rat Hsc70 peptide binding domain (HscPBD) using multi-dimensional NMR experiments. We find that the topology is very different from the predicted topology, even though the location of several secondary structure elements in HscPBD and HLA is found to be quite analogous. We have not been able to identify a similar fold among the classes of protein folds as defined by Thornton and co-workers (Orenga et al., 1993; Orenga & Thornton, 1993), nor does the HscPBD domain fold resemble the peptide binding domain fold of the functionally related chaperone Gro-EL for which the crystal structure was recently determined (Braig et al., 1994).

MATERIALS AND METHODS

Sample. The gene coding for rat Hsc70 peptide binding domain (HscPBD) was under IPTG-inducible T7 promoter control in *Escherichia coli* strain JM109 (DE3). Up to 50 mg/L fully $^{13}C/^{15}N$-labeled pure protein was obtained from M9-media cell cultures containing 1 g/L ^{15}N-labeled ammonium chloride and 2 g/L [^{13}C]-D-glucose (Cambridge Isotopes, Inc.). The peptide sequence $(His)_6$ follows the native HscPBD to allow affinity purification with a Ni column (Qiagen) according to manufacturer's recommendations. This peptide was not removed as we wanted to avoid potential partial degradation of the protein core by the required limited proteolysis. The signals of the $(His)_6$ peptide were found not to interfere with the key NMR experiments needed for structure determination. The peptide binding ability of the obtained HscPBD was confirmed using the methods of Wang (Wang et al., 1993) using peptide A [see Flynn et al. (1989)] as a substrate. The ^{15}N T_2 relaxation time of HscPBD is 60 ms on average, at 1.2 mM concentration, showing that the protein is effectively monomeric (W. Hu and E. R. P. Zuiderweg, unpublished). At 1−1.4 mM protein concentration and 25 °C, amide proton line widths were 20 Hz, well in the range of expected ^1H line widths for a 18 kDa protein but too narrow for a dimeric form of the protein. Slight improvements in hydrodynamic behavior were obtained by using 10% acetonitrile-d_3 (Cambridge Isotopes, Inc.) as a cosolvent; this also resulted in marked improvements in stability of the protein against precipitation, aggregation, and denaturation. The protein solution was kept at pH 7.0 in 50 mM sodium phosphate buffer and 0.02% sodium azide, as we have indications that stability is limited at the for NMR more favorable lower pH values.

NMR Assignments. The NMR signals of $^{13}C\alpha$, $^{15}N\alpha$, and ^1HN nuclei were correlated using 3D HNCA and HN(CO)CA (Ikura et al., 1990; Bax & Grzesiek, 1993) experiments. Degeneracy in the two-dimensional $^{15}N\alpha$ and ^1HN correlations was low, but typically four or five different possibilities were found for each one-dimensional Cα correlation in this assignment pathway. $^1H\alpha$, $^{15}N\alpha$, and ^1HN nuclei were correlated using 3D HN(CA)HA (Clubb et al., 1992) and HA(CACO)NH (Boucher et al., 1992; Van Doren et al., 1993) experiments. Typically four or five different possibilities were found for each one-dimensional Hα correlation in this assignment pathway as well. A computer routine was written to combine the two pathways yielding stretches of 8−10 connected peptide units. All suggested connections were inspected using computer graphics. The assigned peptide fragments were placed in the amino acid sequence utilizing data obtained from cross-polarization-driven HCCH (Majumdar et al., 1993; Wang & Zuiderweg, 1995) and (H)C(CCO)NH (Grzesiek & Bax, 1993; Wang & Zuiderweg, unpublished) spectroscopies. Especially the last experiment was useful, as it gave for most residues virtually complete side-chain carbon chemical shift positions. Assignments were further verified from 3D ^{15}N-resolved NOESY, where strong d_{NN} connectivities in the α-helix and several (very) weak d_{NN} connectivities in more extended regions gave an independent backbone assignment pathway. While the $d_{\alpha N}(i,i+1)$ NOEs that are easily identified in the 3D ^{15}N-resolved NOESY did not ascertain the assignments [these same connectivities are found in the HA(CACO)NH experiment], readily observable $d_{\beta N}(i,i+1)$ NOEs in the 3D ^{15}N-resolved NOESY and sequential NOEs to more peripheral side-chain protons did serve as an independent validation of the triple-resonance-based assignments. Final assignment verification was obtained from a $^{13}C/^{15}N$-labeled sample prepared with [^{12}C]leucine. Using a high-resolution, in-phase ^{15}N-HSQC experiment (Van Doren et al., 1993), in which band-selective Cα decoupling was used during the ^{15}N evolution time, we could identify the NH cross peaks of residues sequentially neighboring Leu residues by the absence of one-bond CO scalar coupling in the ^{15}N dimension.

Secondary Structure Identification. 3D ^{15}N-resolved NOESY, $^{15}N-^{15}N$-resolved NOESY, and ^{13}C-resolved NOESY spectroscopies [see Clore and Gronenborn (1991) for a review] were used for the identification and semiquantification of the $d_{\alpha N}(i,i+n)$ and $d_{NN}(i,i+1)$ NOEs indicated in Figure 1. The same spectra were used to identify the cross-sheet NOEs shown in Figure 2. Amide proton exchange was measured by rapidly exchanging the buffer of the protein in a Amicon dialysis cell and recording $^{15}N-^1H$ correlation spectra every 15 min. The dead time of the preparation was 10 min. Amide proton exchange, recorded at pH 7.0 and 25 °C, was relatively fast. Virtually all protons were exchanged within 2 h of exposure to the ^2H_2O buffer. Nevertheless, a clear differentiation of amide proton ex-

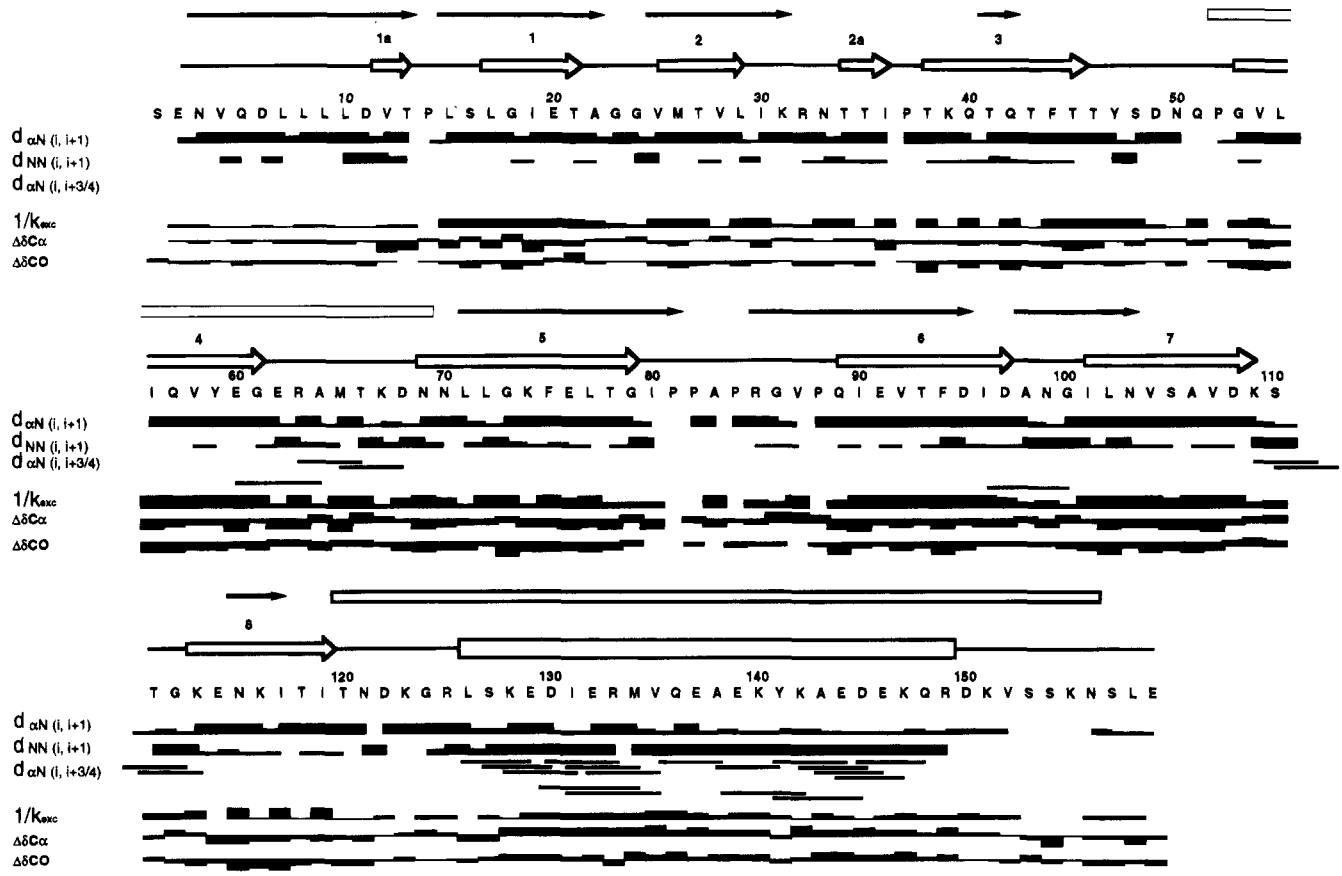

FIGURE 1: Sequence, NMR data, and secondary structure of the heat shock cognate Hsc70 peptide binding domain (HscPBD), pH 7.0, 25 °C, in 90%H_2O/10% acetonitrile-d_3. Sequence-specific assignments were obtained primarily from 3D triple resonance experiments (see text). $d_{\alpha N}(i,i+n)$ NOEs were obtained from 3D ^{15}N-resolved NOESY and 3D ^{13}C-resolved NOESY while $d_{NN}(i,i+n)$ NOEs were collected from 3D ^{15}N-resolved NOESY and 3D ^{15}N−^{15}N resolved NOESY. The $d_{\alpha N}(i,i+1)$ and $d_{NN}(i,i+1)$ NOEs are classified as weak, medium, or strong by the thickness of the bars. Amide proton exchange experiments were performed by rapidly exchanging buffers in a dialysis cell and recording ^{15}N-HSQC spectra every 15 min. The exchange data at pH 7.0 and 25 °C are is displayed as a protection factor ($1/k_{ex}$) with five different categories ranging from slow ($t_{1/2} \sim 30$ min) to fast ($t_{1/2} \sim 10$ min). The deviations of the resonance shifts from random coil position are indicated for ^{13}Cα and ^{13}CO using the compilation of Wüthrich (1976) with an adjustment of +1.6 ppm for referencing against DSS. The differences are plotted as positive or negative deviations in 1 ppm increments. The secondary structure of HscPBD as determined in this study is displayed directly above the sequence. The strands that participate in β-sheet structure (arrows) were identified from interstrand hydrogen bonding as determined by long-range NOEs (see Figure 2) as well as from $d_{\alpha N}(i,i+1)$, slow exchange amide protons, and Δδ Cα and Δδ CO. The helix (box) was identified by the abundance of $d_{NN}(i,i+1)$ and $d_{\alpha N}(i,i+3/4)$ NOEs, slowly exchanging amide protons, and chemical shift deviations. The secondary structure of HLA-A2 (Bjorkman et al., 1987) aligned with HscPBD (Rippmann et al., 1991) is shown with thin arrows for β-strands and boxes for helices in the top lines.

change kinetics over the HscPBD protein could be discerned as indicated in Figure 1. Finally, the Cα and CO shift deviations from random coil values (Wüthrich, 1974) are indicated in the figure as well.

RESULTS AND DISCUSSION

Secondary Structure. The combined data indicate that the secondary structure of HscPBD is mostly extended, except for a long (possibly noncontiguous) helix toward the C-terminus of the molecule. Systematic search for interstrand NOEs (Figure 2) positively revealed a four-stranded antiparallel β-sheet comprising strands 1, 2, 4, and 5 (sheet I) and a four-stranded antiparallel β-sheet comprising strands 3, 6, 7, and 8 (sheet II). Figure 2 shows the abundance of NOEs between the individual strands and also shows the existence of an additional small section of two-stranded antiparallel sheet (1a and 2a). Cα and CO chemical shifts suggest that the peptide dihedral angles and hydrogen-bonding lengths are very regular in strands 4−8 while strands 1−3 must be quite irregular (Spera & Bax, 1991; De Dios et al., 1993; De Dios & Oldfield, 1994). Grid search did not reveal any backbone proton NOEs between the two major four-stranded sheets. Amide proton exchange is moderately and uniformly slow in the central regions of both β-sheets. The exception is a very clear alternating pattern of slower and faster exchange in strands 3 and 8 of the sheet II revealing the solvent exposure of every other amide proton. This validates and explains the absence of cross-strand NOEs for those edge strands. The center of sheet II is amphipathic, suggesting that the sheet forms a protein−solvent boundary (see Figure 2). The situation appears to be less straightforward for sheet I. Amphipathy is less significant, and no clear alternating patterns of slow and fast amide proton exchange are observed for edge strands 2 and 5. It is noted that the residues in strand 2 are mostly hydrophobic (V^{25}, M^{26}, L^{29}, and I^{30} are completely conserved between Hsp70 proteins of human, *Xenopus*, *Drosophila*, yeast, and *E. coli*; Lindquist, 1986), thus suggesting that this part of sheet I is buried or is possibly part of a peptide binding site. The helix is defined to be mostly of the α type by the presence of $d_{\alpha N}(i,i+4)$ NOEs. Judging from Cα and CO shifts, it must have a fairly regular structure, with a possible exception around residue

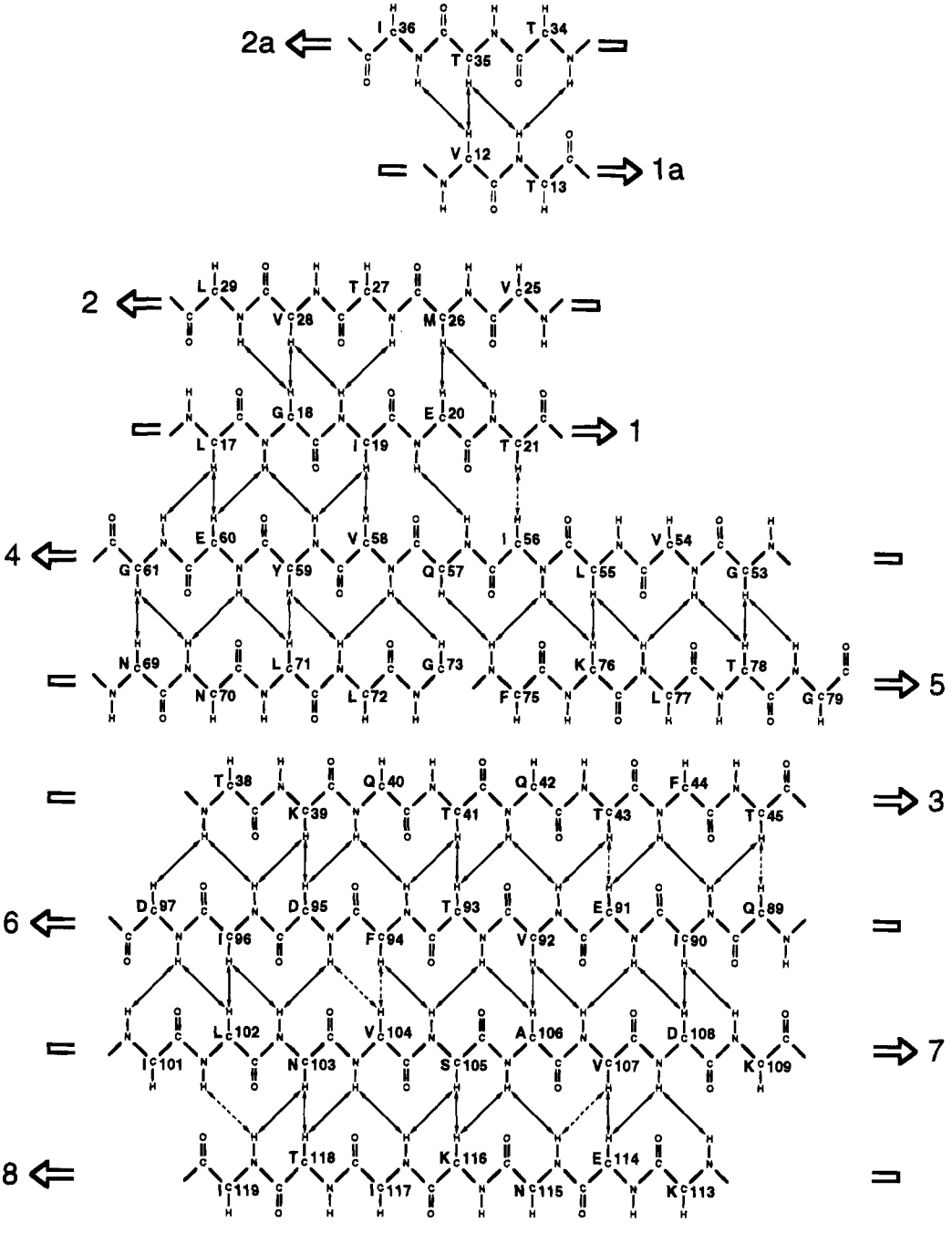

FIGURE 2: β-Sheet topology of HscPBD as determined from long-range NOEs. Observed NOEs are indicated by solid arrows. Absence of arrows indicates that the corresponding NOEs were absent in all spectra while dashed arrows indicate that absence or presence of the corresponding NOEs could not be determined because of overlap in all spectra used. $d_{NN}(i,i+n)$ NOEs were obtained from 3D ^{15}N-resolved NOESY and 3D ^{15}N−^{15}N-resolved NOESY, $d_{\alpha N}(i,i+n)$ NOEs were identified in both 3D ^{15}N-resolved NOESY and 3D ^{13}C-resolved NOESY, and $d_{\alpha\alpha}(i,i+n)$ NOEs were observed in 3D ^{13}C-resolved NOESY.

140. Hydrogen exchange is moderately slow over the entire helix but is significantly faster at residue 142, also suggesting a kink around location 140. The reduction in density of medium-range NOEs spanning this junction also supports this notion. We observe a slightly slower exchange for the amide proton of S^{127} than for that of K^{128}. Hydrogen bonding in the typical N-cap sequence (Harper & Rose, 1993)—the pattern S/T^{127}-XX-D/E^{130} is conserved (Lindquist, 1986)—could explain this observation. The center part of the helix shows conserved amphipathy (I^{131}-XX-M^{134}V^{135}-XX-A^{138}-XX-Y/F/M^{141}; Lindquist, 1986). It is not unreasonable to expect that this part of the helix is docked to the protein core. An irregular turnlike structure exists around residue 65 as is identified by several medium-range NOEs in this region. The N-terminal 10 residues of the protein have extended structure, and their resonances have considerably narrower line widths. This mobility strongly suggests that the N-terminal region is not part of the integral protein body. This is somewhat surprising, since the sequence of very hydrophobic residues in this region (here L^7-L^8-L^9-L^{10}) is conserved (Lindquist, 1986). Possibly, this area has a function in the complete 70 kDa proteins by stabilizing the interaction with the 44 kDa ATPase domain. The C-terminus of the molecule is not as mobile since the NMR lines here are relatively broad, but it appears to be exposed as the amide-proton-based NMR data for this area (e.g., the triple-resonance experiments) are very

weak in intensity. It is possible that the lack of structure in this area is stimulated by the unnatural His_6 tail following residue 159.

Homologies. It has been suggested that the peptide binding domain of the 70 kDa heat shock proteins is related to that of the human leukocyte antigen (HLA) peptide-presenting protein of the major histocompatibility complex, class I, on the basis of related function, limited amino acid homology, and secondary structure prediction (Rippmann et al., 1991; Flajnik et al., 1991). This model has recently gained much credence in light of Wang's finding that Hsc's peptide binding domain is indeed confined to the 18 kDa fragment (Wang et al., 1993) identified by Rippmann as having the highest amino acid homology with HLA sequences. Accordingly, the Hsc peptide binding domain would resemble a "cradle" with two α-helices at the sides and with a single contiguous eight-stranded antiparallel β-sheet as the "mattress". Modeling Hsp70 peptide binding domains as such is not unappealing because both molecules have similar function (peptide binding). Moreover, HLA molecules have been shown to present peptides in a generally extended conformation (Madden et al., 1993; Stern et al., 1994), similar to the peptide binding mode of Hsp class proteins (Flynn et al., 1989, 1991; Blond-Elguindi et al., 1993; Landry et al., 1992; Palleros et al., 1991). It is also found that hydrophobic peptide side chains are sequestered by the binding site in HLA (Madden et al., 1993; Stern et al., 1994) and also conform to expectations of the peptide binding mode of Hsp70 molecules, which bind to hydrophobic peptides (Flynn et al., 1991; Blond-Elguindi et al., 1993). The secondary structure of HLA, aligned with Hsc as suggested by Rippmann, is included in Figure 1. It is obvious that considerable secondary structure homology does indeed exist between the two protein domains. Many of the β-strands are found on approximately the same locations in both molecules, and the position of the long C-terminal α-helix corresponds rather well, too. However, the first HLA β-strand is mostly missing in HscPBD, and the first α-helix of HLA is replaced by a β-strand and a pronounced turn in HscPBD. But, even with these differences, it would not be unreasonable to expect that the folds of the molecules should show at least some similarity, especially in the C-terminal halves of the molecules. That this is not the case follows from the identification of a large number of NOEs between the strands (Figure 2). The comparison (Figure 3) of the topology diagrams of HscPBD (from these data) and of HLA (Bjorkman et al., 1987) shows that not much homology between the molecules exists at this level. The salient difference is that the sheet in HLA is contiguous, whereas HscPBD contains two independent sheets of four strands each. Even the C-terminal half of the molecule, with the compelling analogy in the location of its secondary structure elements, is folded differently in the two molecules; sheets 5−8 in HLA have canonical hairpin structure, whereas in HscPBD strand 5 is located in the other sheet and is replaced by strand 3. Superficially, of course, strands 3/6/7/8 in HscPBD could be termed homologous with strands 5/6/7/8 in HLA if one considers strands 4/5 in HscPBD to be just an extended loop between strands 3 and 6. However, we cannot discern any clear amino acid homology between conserved residues in HLA strand 5 (Rippmann et al., 1991) and HscPBD strand 3 (Lindquist, 1986) that would support

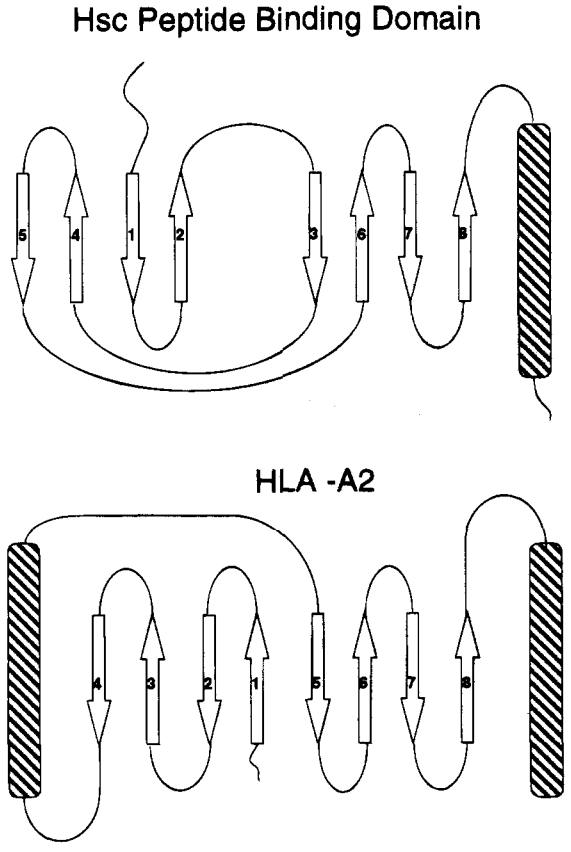

FIGURE 3: Comparison of the secondary structure topology diagrams for the Hsc70 peptide binding domain (HscPBD; this study) and human leukocyte antigen (HLA-A2; Bjorkman et al., 1987).

such a notion. Based on the observations, it would be very surprising to find any homology between HLA and HscPBD on the tertiary level; initial model building suggests that the first and second sheets in HscPBD cannot be put in the same plane and can therefore not resemble the contiguous β-sheet of HLA-A2.

In summary, even though compelling homologies exist between the molecules in the HscPBD and HLA families at the level of function, peptide binding mode, primary structure, and location of secondary structure *elements*, we obtained strong experimental evidence that the secondary structure *topology* is very different between the two families of proteins. At this point, it is worthwhile to reiterate the quality of the experimental evidence we have obtained. The definition of the topology comes from 73 cross-strand NOEs, defined from 3D ^{15}N-resolved NOESY, 3D $^{15}N-^{15}N$-resolved NOESY, and 3D ^{13}C-resolved NOESY. The resolution in these experiments, as well as the internal cross-validation in this large set of NOE identifications, makes it next to impossible to align the strands in the sheets differently than shown in Figure 2. The validity of the topology alignment is thus only dependent on the validity of the NMR resonance assignments. At that level, entire strands could, in principle, have been assigned to incorrect regions of the protein. Such mistakes are not impossible to make if the resonance assignments were to be based on triple-resonance assignments methods alone. We have, however, extensively used 3D HCCH and 3D (H)C(CCO)NH experiments to establish connectivities between the peptide backbone resonances and the side-chain resonances, have validated the assignments from 3D ^{15}N-resolved NOESY spectroscopy [d_{NN} and $d_{\beta N}$-

($i,i+1$) NOEs], and have validated the assignments by studying the NMR spectra of a specially Leu-labeled HscPBD. Taken together, the HscPBD NMR assignments should be correct beyond any reasonable doubt; it follows that the deduced secondary structure topology must also be correct and very different from the HLA topology. We note that the HscPBD topology does not resemble the recently solved structure of the peptide binding domain (the apical domain) of the Gro-EL chaperonin (Braig et al., 1994) either.

Classification. HscPBD should be classified as an $\alpha + \beta$ protein as it consists exclusively of an antiparallel β-sheet and α-helix (Chothia & Finkelstein, 1990). The general topology is not unlike an immunoglobulin β-sandwich, but this exact topology has not been observed among proteins in the protein data bank release of mid-1993 as studied by Thornton and co-workers (Orengo et al., 1993; Orengo & Thornton, 1993) or in the not dissimilar cell surface adhesion receptors (Wagner & Wyss, 1994). In fact, the exact meander fold of the first four-stranded antiparallel β-sheet, characterized by a center-sheet start of a hairpin of strands a and b, an excursion to another sheet, and completion with a hairpin of strands c and d (the pattern d c a b, where a = strand 1, b = strand 2, c = strand 4, and d = strand 5 for Hsc) does not occur at all. Reminiscent patterns are however found in γ-crystallin (Protein Data Bank entry 1gcr) (a center-sheet start of a hairpin of strands a and b, an excursion, strand c, a very large excursion, strand d) and in mannose binding protein (Protein Data Bank entry 1msb) (a center-sheet start of a hairpin of strands a and b, a short connection to strand c, and completion with a hairpin of strands c and d). The topology of the second sheet (a three-stranded hairpin flanked by one or more extraneous strands) is of course much more commonly found.

ACKNOWLEDGMENT

We thank Dr. C. Wang for the gift of the pPBD/hsc70 plasmid and Dr. S. R. Van Doren for advice. Shared instrumentation grants (NIH and NSF) provide support of the 500 MHz NMR system; Parke-Davis−Warner-Lambert Co. is acknowledged for generous support toward the 600 MHz NMR instrument and computer hardware.

REFERENCES

Bax, A., & Grzesiek, S. (1993) *Acc. Chem. Res. 26*, 131−138.
Bjorkman, P. J., Saper, M. A., Samraoui, B., Bennett, W. S., Strominger, J. L., & Wiley, D. C. (1987) *Nature 329*, 506−512.
Blond-Elguindi, S., Cwirla, S. E., Dower, W. J., Lipshutz, R. J., Sprang, S. R., Samrook, J., & Gething, M.-J. (1993) *Cell 75*, 717−728.
Boucher, W., Laue, E. D., Campbell-Burk, S., & Domaille, P. J. (1992) *J. Am.Chem. Soc. 114*, 2262−2264.
Braell, W. A., Schlossman, D. M., Schmid, S. L., & Rothman, J. E. (1984) *J. Cell Biol. 99*, 734−741.
Braig, K., Otwinowski, Z., Hegde, R., Bolsvert, D. C., Joachimiak, A., Horwich, A.L., & Sigler, P. A. (1994) *Nature 371*, 578−586.
Chappell, T. G., Welch, W. J., Schlossmann, D. M., Palter, K. B., Schlesinger, M. J., & Rothman, J. E. (1986) *Cell 45*, 3−13.
Chothia, C., & Finkelstein, A. V. (1990) *Annu. Rev. Biochem. 59*, 1007−1039.
Clore, G. M., & Gronenborn, A. M. (1991) *Prog. NMR Spectrosc. 23*, 43−92.
Clubb, J., Thanabal, V., & Wagner, G. (1992) *J. Biomol. NMR 2*, 203−210.
Craig, E. A., Gambill, B. D., & Nelson, R. J. (1993) *Microbiol. Rev. 57*, 402−414.
De Dios, A. C., & Oldfield, E. J. (1994) *J. Am. Chem. Soc. 116*, 11485−11488.
De Dios, A. C., Pearson, J. G., & Oldfield, E. (1993) *Science 260*, 1491−1496.
Flaherty, K. M., DeLuca-Flaherty, C., & McKay, D. B. (1990) *Nature 346*, 623−628.
Flajnik, M. F., Canel, C., Kramer, J., & Kasahara, M. (1991) *Proc. Natl. Acad. Sci. U.S.A. 88*, 537−541.
Flynn, G. C., Chappell, T. G., & Rothman, J. E. (1989) *Science 245*, 385−390.
Flynn, G. C., Pohl, J., Flocco, M. T., & Rothman, J. E. (1991) *Nature 353*, 726−730.
Gragerov, A., & Gottesman, M. E. (1994) *J. Mol. Biol. 241*, 133−135.
Grzesiek, S., & Bax, A. (1993) *J. Biomol. NMR 3*, 185−204.
Harper, E. T., & Rose, G. D. (1993) *Biochemistry 32*, 7605−7609.
Ikura, M., Kay, L. E., & Bax, A. (1990) *Biochemistry 29*, 4659−4667.
Landry, S. J., Jordan, R., & Gierash, L. M. (1992) *Nature 355*, 455−457.
Lindquist S. (1987) *Annu. Rev. Biochem 55*, 1151−1191.
Madden, D. R., Garboczi, D. N., & Wiley, D. C. (1993) *Cell 75*, 693−708.
Majumdar, A., Wang, H., Morshauser, R., & Zuiderweg, E. R. P. (1993) *J. Biomol. NMR 3*, 387−397.
Orengo, C. A., & Thornton, J. M. (1993) *Structure 1*, 105−120.
Orengo, C. A., Flores, T. P., Taylor, W. R., & Thornton, J. M. (1993) *Protein Eng. 6*, 485−500.
Palleros, D. R., Welch, W. J., & Fink, A. L. (1991) *Proc. Natl. Acad. Sci. U.S.A. 88*, 5719−5723.
Rippmann, F., Taylor, W., Rothbard, J., & Green, N. M. (1991) *EMBO J. 10*, 1053−1059.
Spera, S., & Bax, A. (1991) *J. Am. Chem. Soc. 113*, 5490−5492.
Stern, L. J., Brown, J. H., Jardetzky, T. S., Corga, J. C., Urban, R. G., Strominger, J. L., & Wiley, D. C. (1994) *Nature 368*, 215−221.
Van Doren, S. W., Kurochkin, A. V., Ye, Q. Z., Johnson, L. L., Hupe, D. J., & Zuiderweg, E. R. P. (1993) *Biochemistry 32*, 13109−13122.
Wagner, G., & Wyss, D. F. (1994) *Curr. Opin. Struct. Biol. 4*, 893−901.
Wang, H., & Zuiderweg, E. R. P. (1995) *J. Biomol. NMR 5*, 207−211.
Wang, T.-F., Chang, J.-H., & Wang, C. J. (1993) *J. Biol. Chem. 268*, 26049−26051.
Wüthrich, K. (1976) *NMR in Biological Research: Peptides and Proteins*, North-Holland, Amsterdam.

BI950407U